DTU Library

Assessing bicycle crash risks controlling for detailed exposure

A Copenhagen case study

Myhrmann, Marcus Skyum; Mabit, Stefan Eriksen

Published in:
Accident Analysis and Prevention

Link to article, DOI:
10.1016/j.aap.2023.107226

Publication date:
2023

Document Version
Publisher's PDF, also known as Version of record

Accident Analysis and Prevention 192 (2023) 107226

Contents lists available at ScienceDirect

Accident Analysis and Prevention

journal homepage: www.elsevier.com/locate/aap

Assessing bicycle crash risks controlling for detailed exposure: A Copenhagen case study

Marcus Skyum Myhrmann, Stefan Eriksen Mabit *

Transport Division, DTU Management, Technical University of Denmark, Bygningstorvet, Building 116B, 2800 Kgs. Lyngby, Denmark

ARTICLE INFO

Keywords:
Palm distribution
Cycling
Bicycle crash risk
Disaggregate risk assessment
Adverse weather impact
Accident analysis

ABSTRACT

A better understanding of factors associated with bicycle crashes can inform future efforts to limit crash risks. Many previous studies have analysed crash risk based on crash databases. However, these can only provide conditional information on crash risks. A few recent studies have included aggregate flow measures in their crash risk analyses. This study incorporates detailed bicycle flow to investigate factors related to bicycle crashes. Specifically, the study assesses the relative crash risk given various conditions by applying Palm distributions to control for exposure.

The study specifically investigates the relationship between weather and time conditions and the relative risk of bicycle crashes at a disaggregate level. The study uses bicycle crash data from police reports of bicycle crashes from 2017–2020 in the greater Copenhagen area (N = 4877).

The relations between the bicycle crash risk and the air temperature and wind speeds are found to be highly non-linear. The relative risk of bicycle crashes is elevated at low and high temperatures (0 °C > x, x > 21 °C). The results also show how decreasing visibility relates to increasing bicycle crash risk. Meanwhile, cycling during the early morning peak (7–8) and afternoon peak hours (15–18) is related to an increased risk of bicycle crashes. While some of the effects are likely spurious, they highlight specific conditions associated with higher relative risk. Finally, the results illustrate the increased risk at weekend night times when cyclists are likely to bike under the influence of alcohol.

In conclusion, the analysis confirms that visibility, slippery surfaces, and intoxication are all factors associated with a higher risk of bicycle crashes. Hence, it is relevant to consider how infrastructure planning and preventive measures can modify the bicycle environment to minimise these risks.

1. Introduction

The bicycle, as a means of urban transport, is receiving increased attention due to its appealing benefits of improved urban livability and physical health of the users (Infrastructures, 2015; Mueller et al., 2015; Useche et al., 2018a). Yet, a continuously reported barrier to increasing the number of cyclists is the growing number of crashes along with fear of crashes (Horton, 2016; Transport for London, 2014; Vejdirektoratet, 2018). A better understanding of the factors associated with bicycle crashes can help inform future efforts to limit the crash risk and support the promotion of bicycling.

Traditionally, investigations of factors surrounding any type of road traffic crash are based on records of traffic crashes. Such records provide information on conditions such as weather, road surface, and time of the day, as well as information on the crash itself, e.g. the number of casualties, type of crash, and the crash mechanics. Based on this information, various statistical methods have been employed to identify significant factors related to road traffic crashes (Mannering and Bhat, 2014; Lord and Mannering, 2010). Meanwhile, the significance of a statistical analysis of the crash distribution alone is limited because it provides no information about the normal state of the world outside the crash times (Norros et al., 2016). In the realm of cycling crash analysis, little research has been conducted analysing crash circumstances in light of the cycling traffic/exposure (Dozza, 2017; Vanparijs et al., 2015). One reason could be the limited availability of bicycle volume data (Vandenbulcke et al., 2014). While the discussion above focuses on studies based on police reports, there are other factors that influence bicycle crash risk, e.g. bicycle experience and risk-seeking behaviour. These factors have been studied using other survey instruments. However, independent of survey instrument exposure is fundamental for understanding crash risk since without bicyclists there would be no crashes. Additionally, not accounting for exposure among cyclists can lead to biased results, as it will be unclear if an increase in accidents

* Corresponding author.
E-mail addresses: mskyum@dtu.dk (M.S. Myhrmann), smab@dtu.dk (S.E. Mabit).

https://doi.org/10.1016/j.aap.2023.107226
Received 3 January 2023; Received in revised form 26 May 2023; Accepted 14 July 2023
Available online 18 August 2023

should be attributed to a specific factor or is the result of more cyclists being on the road (Dozza, 2017).

The technologies necessary for detailed measurement of bicycle exposure are increasingly available via systems such as instrumented cyclists (Gustafsson and Archer, 2013; Roos and Lindqvist, 2020; von Stülpnagel et al., 2022), they are still not widespread enough to give representative data for larger urban networks. Various studies have overcome this by using aggregate exposure measures for a limited number of locations, e.g. Miranda-Moreno et al. (2011), who use peak hour aggregates for some intersections to investigate the bicycle crash risk at those locations. Whereas von Stülpnagel et al. (2022) use cycling activities tracked via a smartphone app over a short period to provide relative traffic estimates. A few studies on bicycle risk use more advanced statistical methods, specifically case-control methods, to cover more extensive networks. Vandenbulcke et al. (2014) use a census gathered data to establish the Potential Bicycle Traffic, while Williams (2015) and Aldred et al. (2018) use model-generated aggregate cycling volumes across their respective networks. These studies present some of the most novel research on bicycle crash risk analysis but are reliant on some level of aggregated measures of bicycle traffic and are thus prone to potential aggregation biases.

This study presents a method for the analysis of bicycle crash risk at a more disaggregated level accounting for the "normal state" of traffic, i.e. traffic when no crashes occur, namely the Palm distribution of traffic conditions, pioneered by Norros et al. (2016), who applied it to car crashes. To the best of our knowledge the method has only previously been applied to model car crashes within transport research. Contrasting the case-control method (Aldred et al., 2018; Williams, 2015; Vandenbulcke et al., 2014), which compares locations of crashes with control points of no crashes, the Palm distribution method stems from the theory of count processes. The method allows for the evaluation of various cycling conditions based on a comparison of the distribution of conditions 'seen' by an arbitrary cyclist to that 'seen' by the cyclists subject to a crash. In summary, the Palm approach allows us to investigate whether the relative occurrence of crashes given certain conditions is significantly different from the expected occurrences given the relative volume of cyclists under the same conditions. The value of this approach lies in its ability to tackle the role of exposure in crash analysis and at the same time allow for the analysis to be done at any desired level of disaggregation only restricted by data availability.

Considering the limited literature concerning the riskiness of bicycle crashes given adverse weather (Vanparijs et al., 2015), this study additionally contributes by investigating the relation between bicycle crash risk and weather conditions at a disaggregate level. As an extension to previous literature, this study not only considers first-order effects but also evaluates interactions of multiple factors often neglected in studies applying parametric multivariate models.

Overall, the paper contributes by analysing bicycle crash risks controlling for detailed flow, and consequently improving the knowledge base necessary to counter bicycle crashes and aid the design of preventive measures.

2. Methodology

2.1. Palm distributions for relative risk

The Palm distribution of traffic conditions is adapted from Norros et al. (2016). We apply this approach to describe the relative difference between a crash state, i.e. conditions seen from a bicycle crash, and a normal state, i.e. conditions seen from a realised bicycle trip. For each bicycle trip, we describe the context by a vector of observed conditions $X \in C^{tot}$. A specific set of conditions $C \subset C^{tot}$ consists of specific combinations of conditions, such as various weather characteristics (rain, snow, sun...), hours of the day, days of the week, and levels of precipitation. An example could be the set of all combinations with rain.

As the data used in this study are observed at discrete time points, we use the discrete Palm distribution as described in Eq. (1). The Palm distribution given a set of conditions C, where $X_{r,t} \in C$ is a specific vector of observable conditions (various weather and road conditions) at a discrete time step t and road section r, describes how the conditions seen by a randomly picked cyclist are distributed.

$$\begin{aligned} P^0(C) &= \frac{1}{M} \sum_{r\in\{1..R\}} \sum_{t\in\{1..T\}} M_{r,t} \mathbb{1}(X_{r,t} \in C) \quad \text{where} \\ M &= \sum_{r\in\{1..R\}} \sum_{t\in\{1..T\}} M_{r,t} \end{aligned} \tag{1}$$

where $r \in \{1..R\}$ is an index of the road section being considered, $t \in \{1..T\}$ is an index of the time interval being considered, and $\mathbb{1}(X_{r,t} \in C)$ is an indicator that conditions at road r at time t are part of C. Time intervals are assumed of equal size. M is the total accumulated traffic "mass" and $M_{r,t}$ is the traffic mass at road section r and time t. For the later presentation of the results related to various weather and time-dependent conditions, we consider the following notation: $P^0(C^{x_k})$ will refer to the marginal Palm distribution related to specific weather or time conditions, while $P^0(C^{x_k=x_0})$ will refer to the Palm probability of a weather or time-dependent condition x_k taking on a specific value x_0. As such x_k could refer to an hour-of-the-day variable, and $x_k = x_0$ could refer to the hour of the day being seven in the morning.

Next, we define the empirical crash distribution in Eq. (2). The empirical crash distribution describes a randomly chosen crashed cyclist's average probability of conditions C.

$$\begin{aligned} P^{acc}(C) &= \frac{1}{N_{acc}} \sum_{r\in\{1..R\}} \sum_{t\in\{1..T\}} k_{r,t} \mathbb{1}(X_{r,t} \in C), \quad \text{where} \\ N_{acc} &= \sum_{r\in\{1..R\}} \sum_{t\in\{1..T\}} k_{r,t} \end{aligned} \tag{2}$$

where $k_{r,t}$ is the number of crashes that occurred on road section r in time interval t, while N_{acc} is the total amount of crashes.

2.2. Relative risk and statistical analysis of risk factors

If each cyclist is assumed to have a constant stochastic intensity of being involved in a bicycle crash, then the crash risks would follow the Palm distribution (Norros et al., 2016), specifically if every cyclist has a constant stochastic intensity of being involved in a crash and 5% of cyclist exposure coincides with snowy conditions, we would assume 5% of bicycle crashes to occur under snowy conditions. Applying this idea means that contrasting the circumstance distribution observed at bicycle crashes with the Palm distribution of circumstances hints at the effects of circumstances on crashes.

In this regard, if the variable (i.e. the condition) in question is denoted by C^{x_k}, for example the air temperature, then for each point with value of temperature x_0, we can calculate

$$\frac{P^{acc}(C^{x_k=x_0})}{P^0(C^{x_k=x_0})} \tag{3}$$

These density ratios are estimates of the relative risk increase/decrease when variable (C^{x_k}) takes the value x_0, compared with the overall risk level given by P^0. A ratio of 1 would indicate no change in the relative risk. In contrast, a ratio of 0.8% would indicate a 20% relative risk decrease, and one of 1.5 would indicate a 50% relative risk increase of bicycle crashes, given condition $x_k = x_0$.

We would like to know whether the assertions, we make about the impact of various conditions on the risk of bicycle crashes, could result from pure randomness. To check this, we test if the empirical crash distribution $P^{acc}(C^{x_k})$ could be obtained by random sampling from $P^0(C^{x_k})$ with sample size N equal to the total number of observed crashes ($N = 4487$). If cyclists have a constant stochastic risk of being in a crash, then we would expect the empirical crash probability could be obtained by sampling from the Palm distribution. However, if conditions are strongly associated with the risk of crashes, we would expect a significant difference between the Palm distribution and the empirical crash distribution. We test whether this is the case, by checking if specific condition values $C^{x_k=x_0}$ are observed in $k = NP^0(C^{x_k=x_0})$ bicycle crashes if bicycle crashes follows a Binomial distribution with probability $P^0(C^{x_k=x_0})$ (similar to Norros et al., 2016). If the value $C^{x_k=x_0}$ is observed in k crashes, the upper and lower confidence bounds $[p_u, p_l]$ with significance α are determined by Eq. (4) and computed using the Clopper–Pearson interval (Clopper and Pearson, 1934)

$$\sum_{j=k}^{N}\binom{n}{j}p_l^j(1-p_l)^{n-j} = \sum_{j=0}^{k}\binom{n}{j}p_u^j(1-p_u)^{n-j} = \frac{\alpha}{2} \tag{4}$$

We say that $P^{acc}(C^{x_k=x_0})$ is significantly different from $P^0(C^{x_k=x_0})$ at the α significance level, if $P^{acc}(C^{x_k=x_0}) \notin [p_l, p_u]$. An example of this is shown in the right plot in Fig. 2 at $x_0 = 21$ °C, where the error bars show the confidence interval $[p_l, p_u]$, the blue dot is $P^0(C^{21\,°\mathrm{C}})$, and the red dot is $P^{acc}(C^{21\,°\mathrm{C}})$. If the dot is green, such as $P^{acc}(C^{18\,°\mathrm{C}})$, it means that the crash probability is not significantly different from the Palm probability at the evaluated condition.

2.3. Cycling volume estimation

The computation of the Palm distribution relies on accurate measurements of the traffic flow $M_{r,t}$. Concerning bicycle volume data in Copenhagen, far from all bicycle links in the bicycle network are monitored continuously. Hence, we cannot aggregate the monitored observations in a way similar to Dozza (2017). Therefore we use model-generated hourly bicycle volumes for this study. The model used to produce accurate hourly bicycle volume data for the Copenhagen area network is the Long Short-Term Memory Mixture Density Network (LSTMMDN) proposed by Myhrmann and Mabit (2023). This method is based on a mixture of the Mixture Density Network (MDN) proposed by Bishop (1994), and a Long Short-Term Memory Network (LSTM) (Hochreiter and Schmidhuber, 1997). The model is built, calibrated and validated using bicycle count data from 45 separate bicycle monitoring stations in Copenhagen, recorded from 2017–2020. The model is specifically designed to retrospectively estimate hourly bicycle volume data conditional on the year-aggregated daily cycling traffic on a road section, weather data (such as precipitation volume, visibility, temperature, etc.), and time related information. In total, the model is calibrated using 42,265 hourly bicycle counts and validated on 19,399 hourly bicycle counts. For further information on the statistical model and calibration procedure, we refer to the work (Myhrmann and Mabit, 2023).

For the purpose of deriving the Palm distribution we estimate the cycling volume $M_{r,t}$ at each index r, t. To do so, we need year-aggregated daily cycling data for the sections $r \in R$. The year aggregated data cycling volumes were provided by the PI of the article (Paulsen and Nagel, 2019). These volumes are derived using the Copenhagen Model for Person Activity Scheduling (COMPAS) (Prato et al., 2013). The COMPAS model produces daily activity plans for a synthetic population of the areal. Using the activity plans, a loading model assigns agents on the cycling network in accordance with Paulsen and Nagel (2019), and the aggregated daily loading on each link is then fed into the previously described LSTMMDN to derive hourly cycling flow reflecting external conditions and time effects.

3. Empirical setting: Crash risk in greater Copenhagen

The empirical case examined in this paper relates to the bicycle crash risk in the Copenhagen area in the period 2017–2020. The bicycle crash data are from police reports from the same period. The hourly bicycle volume data are generated with the previously described LSTMMDN model, using COMPASS generated mean day cycling traffic and weather data obtained from the Danish Meteorological Institutes open data API (DMI, 2021).

3.1. Crash data

To establish the empirical bicycle crash distribution P^{acc}, we rely on bicycle crash data obtained from police reports concerning crashed bicyclists in the Greater Copenhagen area from 2017–2020. The area is pale blue in Fig. 1. A zoom-in on the map would show that accidents are mainly along larger roads. Since we do not analyse the build environment this does not affect our analyses. There are missing records in the weather data, amounting to 316 missing hours in January, 586 in February, 597 on March, 19 in April, 177 in May, 607 on June, 17 on July, 25 in August, 571 in September, 432 in October, 220 in November, and 372 in December. And therefore the same periods of hourly bicycle volume estimates cannot be predicted by the LSTMMDN. These missing records result from missing complete months or weeks in the weather data and imputing them is difficult and outside the scope of this paper. Considering the Palm distribution in Eq. (1), using the current bicycle volume data straightforwardly would result in skews in the Palm distribution. This problem will need to be addressed, as not doing so could lead to biases in the computations of the relative risk of bicycle crashes. In order to address this issue, we decided to down-sample the data using bootstrapping with no re-sampling. This way we can ensure an even and more robust distribution of the bicycle volume and weather data, similar to the distribution in a normal year. Specifically as we are missing equivalents of one entire month for the months with the most missing data, we down-sample the weather and bicycle flow data to a three-year sample (~26 280 h of bicycle counts per road section), conditional on the month, day of the week, and daytime of the records. Comparing the mean traffic flow conditional on the seasons and daytime, with and without the bootstrapping procedure, supports this.

Descriptive crash characteristics are shown in Table 1. We see that of the total number of registered bicycle crashes ($N = 4877$), most of the bicycle crashes are bicycle–motor-vehicle crashes (88.8%) and in declining order bicycle–bicycle, bicycle–pedestrian and single-bicycle crashes. Of the crashes, 0.7% resulted in fatal injuries, 19.8% resulted in severe injuries, 9.2% resulted in minor injuries and the remaining 70.3% resulted in ‘no evident injuries’. May, June, August, September, October and November had the most crashes (9% – 10% of the crashes respectively). The remaining months each accounted for 6% – 7% of the crashes. The crash locations are marked with red dots in Fig. 1. Based on the time and place of a bicycle crash, the weather observations from the nearest weather stations (marked with green in Fig. 1) are assumed to be the weather conditions present during the crash.

The reason for considering a larger area for the crashes is to improve the statistical power of the relevant analyses. Norros et al. (2016) discuss how the statistical power of the analysis is affected by the number of crashes in the study. Low crash numbers can affect the inference regarding the significance of the difference in P^{acc} and P^0 as small changes in an already low number of crashes can result in potentially large relative changes. Meanwhile, the LSTMMDN is trained to generate cycling flow dynamics for Copenhagen; the area outlined in black in Fig. 1. However, we believe that the flow dynamics related to changing weather conditions are similar between Copenhagen and the surrounding area. Therefore, we consider the inclusion of the area surrounding Copenhagen reasonable. We also believe that many commuter cyclists travel to and from central Copenhagen and would be included in the city bicycle flow, but potentially have a crash in the Greater Copenhagen area.

3.2. Crash risk assessment

The bicycle crash risk associated with a specific dimension C^{x_k} will be evaluated by computing the density ratio between the empirical crash distribution $P^{acc}(C^{x_k})$, and the Palm distribution $P^0(C^{x_k})$. This relation describes the relative risk profile of having a bicycle crash

Table 1
Descriptive statistics of weather and bicycle data in the period 2017–2020.

Weather categories			
Variable	Frequency	Variable	Frequency
Precipitation			
0 mm	0.957	0–0.1 mm	0.020
0.1–0.2 mm	0.011	0.2–0.3 mm	0.005
0.3–0.5 mm	0.004	0.5–1 mm	0.002
>1 mm	0.001		
Wind strength			
Calm	0.038	Fresh breeze	0.015
Gentle breeze	0.305	High winds	0.000
Light air	0.152	Light breeze	0.380
Moderate breeze	0.109	Strong breeze	0.001
Visibility (Fog density equivalent)			
Clear (>10 km)	0.859	Light haze (4–10 km)	0.111
Haze (2–4 km)	0.021	Thin fog (1–2 km)	0.004
Light fog (0.5–1 km)	0.002	Moderate fog (0.2–0.5 km)	0.001
Thick fog (0.05–0.2 km)	0.001		
Continuous variables	Mean	Std. Dev.	
Temperature (°C)	10.29	6.63	
Crash types (N = 4877)			
Variable	Frequency	Variable	Frequency
Single-bicycle	0.019	Bicycle–bicycle	0.055
Bicycle–pedestrian	0.038	Bicycle–motor-vehicle	0.888

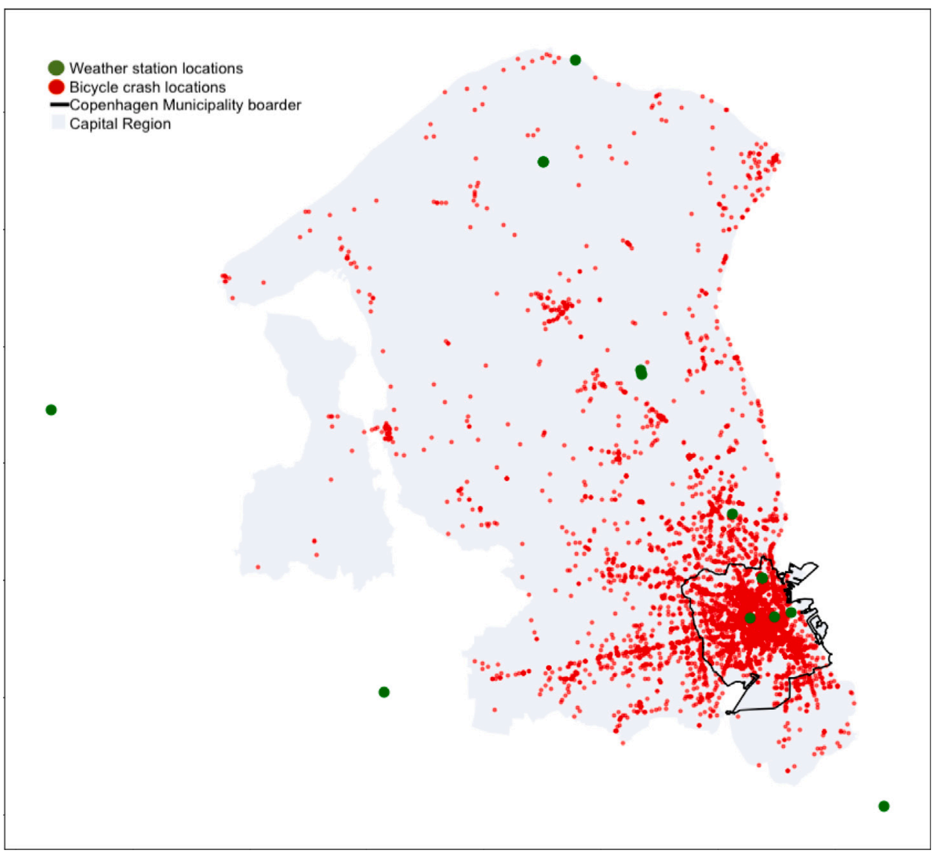

Fig. 1. Locations of the weather measuring stations (in green) and the bicycle crashes (in red). The grey area shows the capital region (greater Copenhagen) while the bounded black section shows the municipality of Copenhagen. (For interpretation of the references to colour in this figure legend, the reader is referred to the web version of this article.)

given conditions C evaluated at specific values $C^{x_k=x_0}$. The significance of the risk change related to the specific values $C^{x_k=x_0}$ will be assessed by establishing whether $P^{acc}(C^{x_k=x_0})$ falls within the $1-\alpha$ central confidence intervals of $P^0(C^{x_k=x_0})$ given N observed crashes as described in Section 2.1 using significance level $\alpha = 5\%$. We use the significance level $\alpha = 5\%$ for the remainder of the paper when discussing significance.

The specific conditions investigated in the risk assessment are the following: Air temperature (grouped into 3 °C increments starting at 0 °C), precipitation amount (in mm), wind speed (on the Beaufort scale), visibility (in km), the hour of the day, day of the week. Meanwhile, previous research has pointed out that increased riskiness is often not just the result of a single condition but the interaction of several. Therefore, we will also investigate the relative risk change

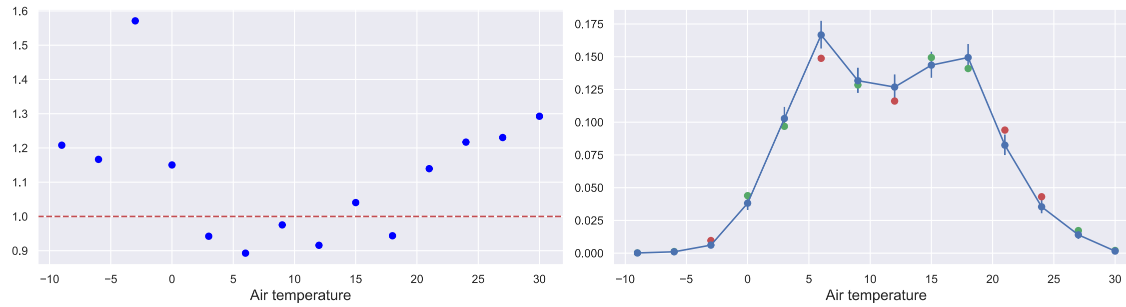

Fig. 2. Left: The relative bicycle crash risk profile given the air temperature as described by the density ratio between the empirical crash distribution and the Palm distribution (blue), line indicating no relative change (red). Right: The Palm distribution of air temperature (blue) and the empirical crash distribution of air temperature (red/green). (For interpretation of the references to colour in this figure legend, the reader is referred to the web version of this article.)

conditional on the interaction between the hour of the day and weekends as well as working weeks, respectively, precipitation and wind speed, precipitation and seasons (astronomical seasons), and freezing temperatures and precipitation.

4. Results

To find crash risks, we calculate the density ratio $\frac{P^{acc}}{P^0}$ for various conditions C^{x_k}. The results are presented for specific conditions using visual approaches as shown in Fig. 2. On the left plot of the figure, we see the density ratios marked with blue dots describing the relative risk profile, $\frac{P^{acc}(C^{x_k=x_0})}{P^0(C^{x_k=x_0})}$, given the dimension C^{x_k}. In Fig. 2, C^{x_k} is related to air temperatures. The blue dots show the relative risk to the specific air temperatures in the left plot. For reference, a red dashed line is plotted, indicating a relative risk ratio of 1. In the right plot, we show the difference in $P^{acc}(C^{x_k=x_0})$ and $P^0(C^{x_k=x_0})$ for the specific values (air temperatures). The blue dots show the Palm probabilities and the red and green dots show the empirical crash probability. The error bars indicate the confidence interval associated with overall risk given each conditional value $x_k = x_0$. The colour of the crash probability marker is there to aid in assessing whether or not the empirical crash probability is significantly different than the Palm probability. I.e. the red dots in the right plot is outside the error bars. In that case, we assess there to be a significant difference between $P^{acc}(C^{x_k=x_0})$ and $P^0(C^{x_k=x_0})$, and hence the change in relative risk at value x_0 will be considered significant.

4.1. Air temperature

The relative risk of bicycle crashes given changing air temperature is described for temperature groupings of 3 °C degree increments as seen in Fig. 2. The density ratio on the left of Fig. 2 reveals a non-linear relation between the relative risk of bicycle crashes and air temperature. We find that temperatures ≤0 °C and ≥21 °C are related to increases in the risk of bicycle crashes of ≥10%. Examining the right plot of Fig. 2, we see the Palm distribution with confidence intervals (error bars) for the air temperature in blue and the empirical crash distribution as red/green dots. If the dot is red, it lies outside error bars, either above or below, we assert that the empirical crash probability and Palm frequency at this point are significantly different. As such, we assert that the temperatures −3 °C, 0 °C, 21 °C, and 24 °C are related to significant increases in the risk of bicycle crashes. More extreme temperatures have similarly elevated risk levels but are not found to be significant. We speculate that this is probably due to the lower number of observations in these conditions.

4.2. Precipitation

The average 10-min intensity of precipitation is grouped to investigate the impact on the relative bicycle crash risk. The profile visualising the relative bicycle crash risk given the precipitation intensity is shown in Fig. 3. No rain is left out of the visualisation as the Palm frequency was 90% (i.e. 90% of bicycle flow occurred in no rain).

The only specific grouping of 10-min average rain intensity in Fig. 3 related to a significant change in the relative risk of bicycle crashes is (0−0.1] mm of rain. While there is a relative increase in the crash risk of bicycle crashes observed at (0.1−0.3] mm, and (0.5−1] mm of rain also, these are not significantly different from the Palm distribution. While not shown in Fig. 3, grouping all rain intensities, comparing cycling in rain with no rain also shows that cycling in rain overall is related to a significant increase in the risk of bicycle crashes.

4.3. Wind speed

Similar to the relative risk profile of air temperature, the relative risk profile related to wind speed exhibits a highly non-linear relation to the wind speed. This is clearly visible by the bathtub shape of the relative risk profile shown in the left-side plot in Fig. 4. With the exception of Light breeze and fresh breeze all grouped wind conditions are related to significant changes in the relative risk of bicycle crashes. Specifically we see that light wind conditions, Calm (<0.2 m/s) and Light air (0.2 m/s−1.5 m/s), as well as Strong breeze (10.7 m/s−13.8 m/s) are related to increased crash risk, while Gentle breeze (3.3 m/s−5.4 m/s) and Moderate breeze (5.4 m/s−7.9 m/s) are related to decreased crash risk.

4.4. Visibility

The average 10-min visibility is grouped to investigate the impact of decreasing visibility on the relative bicycle crash risk. This variable is of considerable importance, as it is one of the weather conditions that most likely affects car drivers and cyclists similarly.

The profile visualising the relative bicycle crash risk given decreasing visibility is shown in Fig. 5. Clear visibility is left out as the Palm frequency was 88% (i.e. 88% of bicycle flow occurred in clear visibility). The results reveal a monotonous increase in the risk of bicycle crashes as the visibility decreases. The visibility being below 2 km is related to a risk increase of ∼125% and the visibility being <0.5 km is related to a risk increase of ∼300%, compared to the Palm distribution. Inspecting the significance by the right plot in Fig. 5, we find that the relative risk increases are significant for all inspected visibility values.

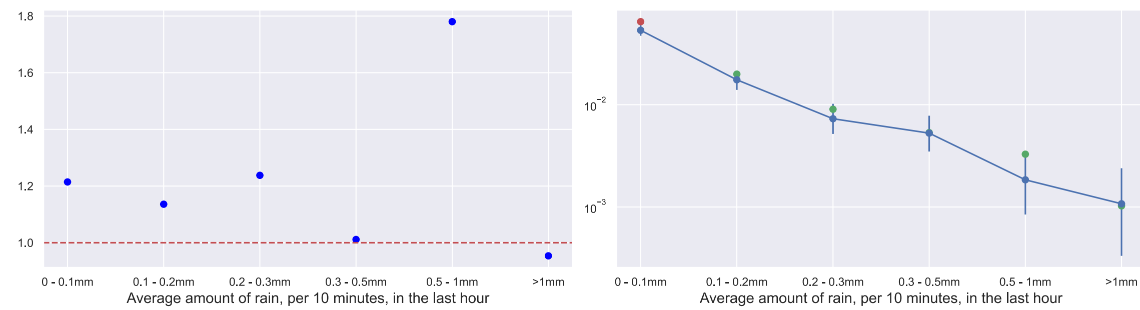

Fig. 3. Left: The relative risk profile of bicycle crashes given varying levels of precipitation. Right: Significance testing of the impact of various precipitation levels.

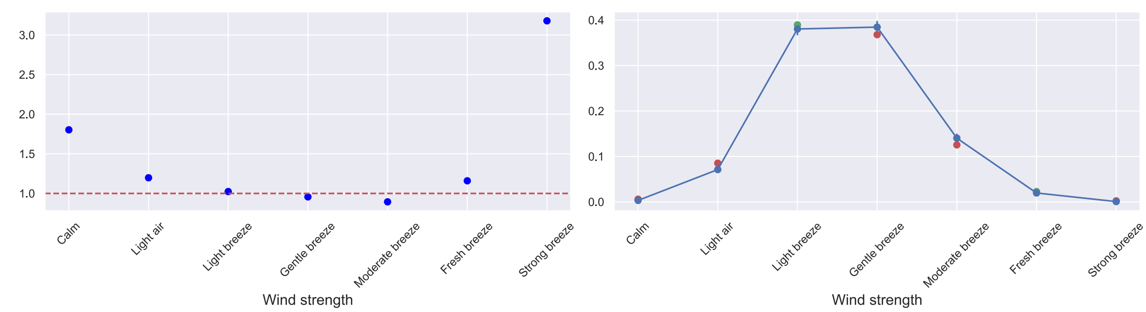

Fig. 4. Left: The relative risk profile of bicycle crashes given the wind speed. Right: Significance test of the impact of wind speed.

Fig. 5. Left: The relative risk profile of bicycle crashes given decreasing visibility. Right: Significance test of the impact of impaired vision.

4.5. Time of day

Fig. 6 shows the relative risk profile and significance tests associated with the hours of the day when averaged over the whole data collection period. The hour of the day values in Fig. 6 are presented as the intervals $(h-1, h]$, i.e. the relative risk for the hour 22–23 is denoted 23. In the left plot in Fig. 6, we see that cycling during evening is related to a significant decrease in the relative risk of bicycle crashes. Meanwhile, peak hours, specifically 7–8 (i.e. the early morning peak) and 15–18, are related to significant increases in the relative risk of bicycle crashes. The increased risk of bicycle crashes in the early morning peak amounts to around 30%. The afternoon peak hours are related to a crash risk increase of 20–30%, relative to the Palm distribution. Inspecting the right plot in Fig. 6, we find that the empirical crash probability P^{acc} is slightly higher in the period 7–8 than the period 8–9. Meanwhile, the cycling exposure P^0 is higher 8–9 than 7–8.

4.6. Day of the week

Fig. 7 shows the relative risk of bicycle crashes for each day of the week. We see a slight increase in the relative crash risk on Tuesdays and Wednesdays and a slight decrease on Mondays and Thursdays. However, no significant change is associated with the differences in P^{acc} and P^0 for the days being Monday, Tuesday, Wednesday or Thursday. Meanwhile, the results show that cycling on Fridays is related to a significant increase in the risk of a crash and weekends are related to a significant decrease in the risk of a crash.

4.7. Time of the day vs. weekday and weekend

Inspired by the analysis in Dozza (2017), we also investigate the relative risk of bicycle crashes as a function of the daytime conditional on weekdays/weekends. The results for weekday daytime riskiness and weekend daytime riskiness are shown in Figs. 8 and 9, respectively.

From the left plot of Fig. 8, we see that the weekday relative risk related to time of day increases at peak hours and presents a different risk profile than the previous average week, see Fig. 6. The increased risk of bicycle crashes in the weekday afternoon peak surpasses that of the morning peak and is related to an approximate increase of 40% between 16 and 17.

The relative risk of bicycle crashes during weekend night time, shown in Fig. 9, is much different from the previous average week shown in Fig. 6. Cycling between midnight and 5 during weekends is related to an increased risk of bicycle crashes compared to the expected risk. However, only the weekend times 0–1 and 3–4 have a significantly increased relative risk of bicycle crashes.

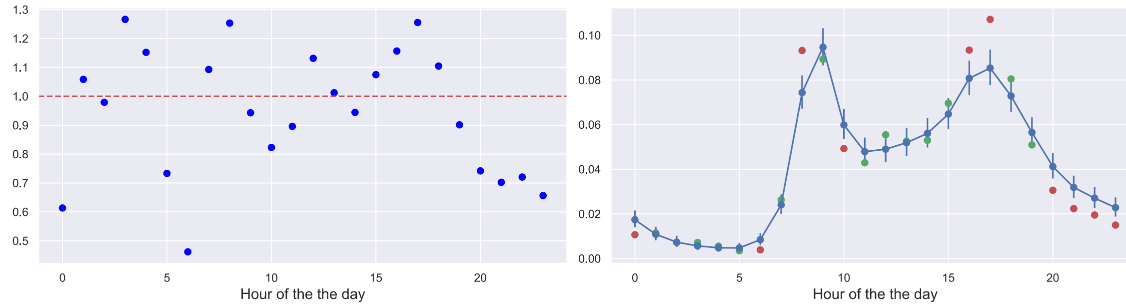

Fig. 6. Left: The relative risk profile of bicycle crashes for the hour of the day, with intervals presented as $(h-1, h]$. Right: Significance test of the impact of the hour of the day.

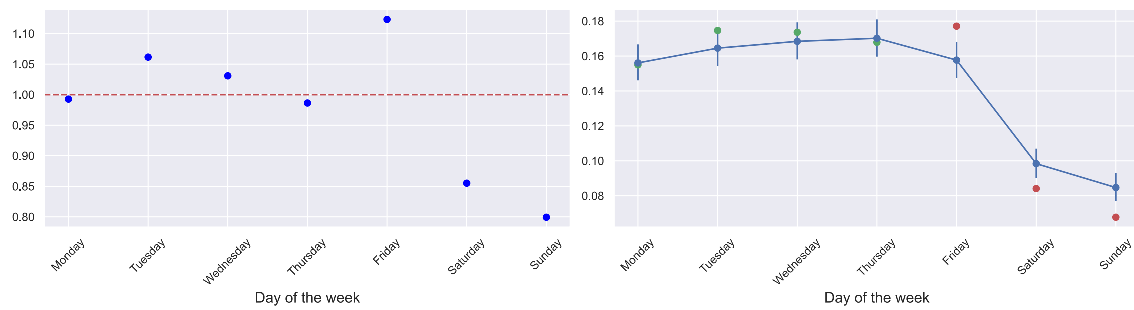

Fig. 7. Left: The relative risk profile of bicycle crashes for the day of the week. Right: Significance test of the impact of the day of the week.

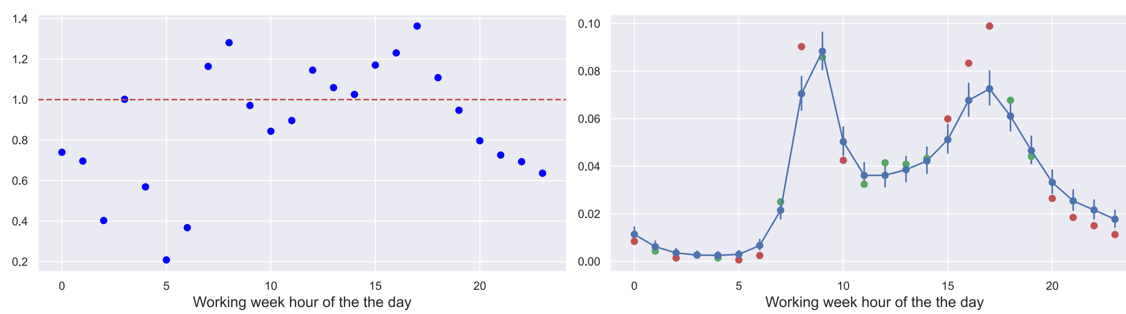

Fig. 8. Left: Relative risk profile for bicycle crashes for the weekday hour of the day. Right: Significance test of the impact related to the weekday hour of the day.

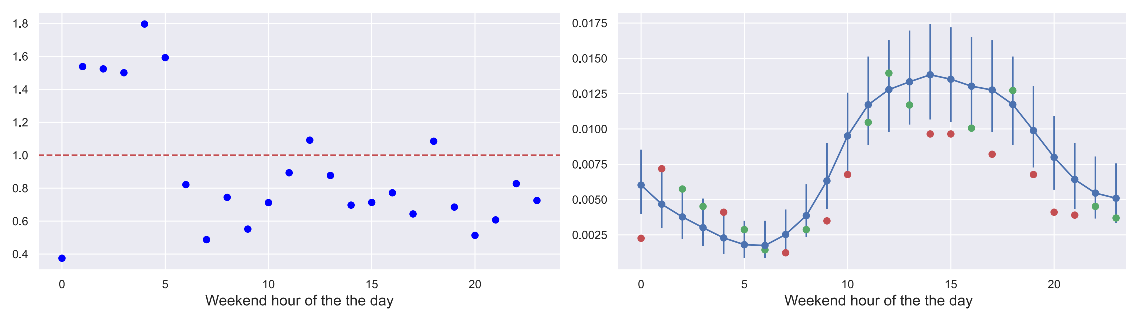

Fig. 9. Left: Relative risk profile for bicycle crashes for the weekend hour of the day. Right: Significance test of the impact related to the weekend hour of the day.

4.8. Further interactions and second-order effects

The Palm distribution for bicycle crash risk can easily investigate potential second-order effects related to interactions between conditions. Therefore we investigate the relative change in bicycle crash risk given interacting weather conditions. Specifically, we investigate the relative risk of bicycle crashes associated with the interactions between astronomical seasons and precipitation, wind speeds of moderate strength or higher (windy conditions) and precipitation, and freezing temperatures and precipitation. Table 2 shows the results for various interactions.

Concerning the seasons, we find that only winter and spring have significant impacts on the relative risk of bicycle crashes. Windy conditions are related to a non-significant relative risk decrease. However, when it is simultaneously raining, the interaction of windy conditions and precipitation results in a significant risk increase of 30%, compared to the Palm distribution. The results reveal that the interaction of freezing temperatures and precipitation is another highly non-linear

Table 2
Results of the various interacting conditions. Bold relative densities indicate a significant difference between the accident and Palm probability.

	Palm frequency	Relative density
No precipitation	0.914	**0.981**
Precipitation	0.086	**1.200**
Autumn	0.261	1.072
Spring	0.251	**1.015**
Summer	0.297	0.980
Winter	0.192	**0.912**
Autumn & No precipitation	0.231	1.046
Autumn & Precipitation	0.030	**1.278**
Spring & No precipitation	0.240	**1.019**
Spring & Precipitation	0.011	0.945
Summer & No precipitation	0.276	0.960
Summer & Precipitation	0.021	**1.229**
winter & No precipitation	0.167	**0.872**
Winter & Precipitation	0.025	1.193
Not windy	0.840	1.011
Windy	0.160	0.943
Not windy & No precipitation	0.766	0.994
Not windy & Precipitation	0.074	**1.181**
Windy & No precipitation	0.148	**0.913**
Windy & Precipitation	0.012	**1.299**
Not freezing	0.955	**0.990**
Freezing	0.045	**1.211**
Not freezing & No precipitation	0.871	**0.975**
Not freezing & Precipitation	0.084	**1.146**
Freezing & No precipitation	0.043	1.101
Freezing & Precipitation	0.003	**2.870**

interaction. The combined effect of precipitation and freezing temperatures results in a risk increase of $\sim$187%. Meanwhile, the average marginal increase of the relative risk of bicycle crashes related to either freezing temperatures or precipitation are $\approx$20%.

5. Discussion and conclusion

This paper presents the results of applying a Palm distribution approach for weather and traffic conditions to evaluate bicycle crash risk. Contrasting earlier work regarding bicycle crash risk (Aldred et al., 2018; Williams, 2015; Vandenbulcke et al., 2014), this study use model-based hourly bicycle volume data to overcome the insufficient monitoring of bicycle traffic while addressing the potential biases associated with using aggregated cycling data. In light of the possible confounding effects of weather and time on bicycle ridership and the risk of crashes, the model for bicycle volume generation reflects the ridership as a function of weather and various time-dependent events. In combination with the Palm distribution for risk assessment, this allows us to provide evidence of several external factors being associated with changes in the relative crash risk of cyclists. In this section, we will in turn discuss the most interesting results: first the specific results on weather effects, second the specific results on time effects, third the results on interactions, and finally we make an overall conclusion on the results. While many of the results could be transferable to other countries, it is important to note that our data stem from a highly developed bicycle culture that is furthermore supported by good bicycle infrastructure in the study area. Therefore some conclusions could be context specific and even though we do find similarities in results with a neighbouring country in Dozza (2017), other countries have less similarity to our Copenhagen case.

5.1. Weather effects

Some of the results on weather effects align with existing literature, e.g. temperature and precipitation. Concerning precipitation, previous findings tie slippery road surfaces to an increase in the number of bicycle crashes (Vanparijs et al., 2016) and car crashes (Malin et al., 2017). The non-linear relation between bicycle crash risk and temperature is in line with previous findings concerning car crashes. Malyshkina et al. (2009) found that extreme temperatures (i.e. cold and warm) correlated with more car crashes. The colder weather could impact the breaking ability of both cars and cyclists and impair cyclist mobility. The relative risk change, given air temperature, seems to align with the findings by Dozza (2017), showing an increased risk of bicycle–motor-vehicle crashes in the winter months.

The reason for the observed increase in the relative risk of bicycle crashes at higher wind speeds could be tied to a plethora of reasons. High wind speeds could impact cyclists' ability to control their bicycles, making uncontrolled interactions with motorised traffic more likely. Meanwhile, the increased risk at low wind speeds is much more difficult to explain. The elevated risk in these conditions might be tied to self-selection because less experienced bikers decide to bike in calm weather, and these riders are more prone to accidents.

Notably, the Palm distribution allows for the identification of an increased bicycle crash risk given ever-decreasing visibility. The results related to visibility show that ever-decreasing visibility leads to an increased relative crash risk. This finding indicates a need for improved street lighting and making cyclists visible (reflective wear) to avoid the high risk of collisions in adverse visibility. It is in line with previous findings suggesting visibility as a significant risk driver in rainy conditions (Andrey and Yagar, 1993). However, it is questionable whether it is a direct effect of visibility less than 10 km or 4 km that causes the higher relative risk or whether, the lower visibility is associated, e.g. with rain, causing more slippery road surfaces. Beyond visibility's impact on cyclists' ability to detect objects and avoid crashes, car drivers' ability to see cyclists could be equally impaired. This has also previously been tied to a higher likelihood of car crashes (Norros et al., 2016; Yu et al., 2013), as well as more severe injuries (Abdel-Aty et al., 2011). A recent study also connects low visibility with an increased risk of severe cyclist injuries in crashes with motorised vehicles (Asgarzadeh et al., 2018).

5.2. Time effects

Car traffic in Copenhagen peaks in the period 7–9 (TomTom International BV, 2021). Meanwhile, cycling traffic peaks at 8–9 (see Fig. 8). Hence the increased riskiness of bicycle crashes from 7 to 8 that is not present from 8 to 9 could illustrate safety in numbers (Elvik, 2009; Elvik and Bjørnskau, 2017). This theory describes the decreasing likelihood of bicycle crashes involving motorised vehicles when the number of cyclists increases relative to the number of cars. This effect is nicely visualised in Aldred et al. (2018). The increased relative risk of bicycle crashes during the afternoon peak could be related to people being tired and unfocused on their way home after work, as being tired and sleepy has previously been linked to increased crash risk (Heaton, 2009; Pack et al., 1995).

Similar to the results in Dozza (2017), the results in Fig. 7 indicate vastly different risk profiles when comparing the weekday and weekend profiles. Therefore, we investigate the relative risk of bicycle crashes as a function of the daytime conditional on weekdays/weekends. Interestingly, the result on relative risk for weekends (see Fig. 9) correlates with the times at which the typical Danish bars and bodegas close. As such, the increase in risk at these hours of the weekend potentially captures people on their way home from bars being possibly intoxicated. This assessment seems to align with previous findings, relating intoxication to an increased frequency of bicycle crashes (Møller et al., 2021; Næss et al., 2020).

Overall, the separation of weekday and weekend provides relevant insights into cycling riskiness that would easily be overlooked in studies using aggregated exposure. Comparing the separation of weekday and weekend risk profiles to the average daytime risk profile highlights how aggregating our data, as in Fig. 6, can lead to an inference that hides the heterogeneity seen in the more disaggregate case. As such, the results concerning the relative risk changes given the hour of the day on weekdays and weekends illustrate the possible knowledge loss that can occur when only considering marginal effects.

5.3. Interactions

The final consideration of the interacting effects is motivated by bicyclists being more exposed to the environment than cars. Hence, many potential interaction effects could be present. Exposure to precipitation on a bicycle not only impairs visibility and surface grip but also impairs the cyclist's mobility. Like cycling in cold weather, cyclists in rainy weather might take a more compact position on the bike, limiting their mobility. Several interesting interaction patterns are revealed in Table 2. For example, cycling in no precipitation during spring is related to an increased relative risk of bicycle crashes. In contrast, cycling in precipitation during spring is related to a decreased relative risk of bicycle crashes. Indeed, this is unexpected if we only consider the first-order effects of each condition separately. At its core, it is a rather curious finding that could reflect that many people start cycling again in the spring, but only in the dry ("good weather"). Meanwhile, the more experienced cyclists, who cycle in the winter, will also cycle in the wet. Hence the lower relative risk of bicycle crashes in spring and precipitation.

5.4. Conclusion

The Palm approach offers a novel approach to include exposure into the analysis of bicycle crash risk. It has been previously used on car crashes. However, the paper illustrates that through proper use of various data sources, it is possible also to apply the approach to bicycle crashes. The non-parametric nature of the Palm distribution approach allows us to identify non-linear effects taking exposure into account. Finally, it provides a straightforward evaluation of various conditions' first- and second-order effects on bicycle crash risk. The results show how various weather and time conditions are significantly associated with variations in the risk of bicycle crashes. The results related to the interaction of several conditions reveal the potential of the Palm distribution to explore interactions. Overall, the non-parametric nature of the Palm provides a valuable complement to established analysis methods through its application ease and visual inspection ability and should be considered for the potential screening of variables and interaction terms due to its ability to identify non-linear effects in the exposure-response relations.

Concerning the identified risk changes given time and weather, it is clear that politicians and city planners cannot influence these circumstances directly. However, they can influence the built environment, lighting, and create awareness campaigns. Like cars having to turn on their lights in rainy conditions, so could street lamps. The lack of street lighting has previously been linked to more severe injury outcomes from bicycle–motor-vehicle crashes (Kim et al., 2007; Asgarzadeh et al., 2018). Resurfacing bicycle lanes could improve braking ability and friction under wet and freezing conditions. Campaigns for high-visibility clothing could potentially mitigate the risk of bicycle–motor-vehicle crashes related to impaired visibility. However, this is speculation on our part and has not been confirmed in any research that we know. Vanparijs et al. (2015) notes that earlier studies did not find any reduction in relative risk from visible clothing. Furthermore, a reduction of car speed limits under inclement weather (rain, low visibility) and peak traffic hours could potentially help mitigate the risk of crashes and has previously been linked to a lower cycling injury risk (Aldred et al., 2018).

6. Limitations and future work

6.1. Heterogeneity

Previous research on accident risks has analysed several important dimensions related to bicycle crash risk, e.g. age and gender (Dozza, 2017; Useche et al., 2018b). However, our bicycle flow data do not include these dimensions, making it impossible to analyse this type of heterogeneity in the present research, similarly for unobserved heterogeneity. The Palm distribution is not set up to account for heterogeneity arising from unobserved differences in cyclists. An example of such unobserved heterogeneity could be heterogeneous ridership. Adverse weather not only impacts the ridership levels but potentially also the composition of the ridership in terms of age and gender distribution, experience, and risk-seeking behaviour. Using the current approach for estimating bicycle volumes does not control for these variations. This connects to the general issue of self-selectivity, as the relative risk profiles might change with the composition of the ridership. For example, the riskiest riders could continue riding in adverse weather. As such, the increased risk at low temperatures is potentially not only due to weather effects (decreased friction, impaired cyclists) but due to the riders in cold weather having fundamentally higher crash rates relative to the overall riding population (Mannering et al., 2020). Meanwhile, the cyclists cycling in the colder weather could equally be the riders who ride all year and are, therefore, the most proficient cyclists. Also, almost 90% of the crashes occur in collision with motorised vehicles, which are the specific transport being discussed in Mannering et al. (2020) and the increased crash risk in adverse weather, could be entirely the fault of risky motorised vehicle drivers. For example, the increased riskiness of bicycle crashes in adverse weather such as <0 °C is most likely a combination of factors like decreased friction, lower rider performance and the increased proportion of risky drivers and cyclists. Similarly, self-selection could play a role in the results related to the Spring season, calm wind conditions, and weekend nights at 1 and 4.

6.2. Police recorded bicycle crashes

The use of police records for performing the risk analysis of bicycle crashes leaves much to be desired in reporting. Police records are severely prone to under-reporting of bicycle crashes (Janstrup et al., 2016). The under-reporting is especially severe for single-bicycle crashes, which is important as these tend to make up 50% or more of the bicycle crashes recorded at emergency departments in Denmark (Myhrmann et al., 2021; Danmarks Statistik, 2021). When comparing the crash risk patterns for single-bicycle crashes and collisions with motorised vehicles, it becomes clear that there are different crash-time distributions. Hence, future studies should consider other more representative data sources, e.g. emergency department data.

6.3. Further research

The limitations above highlight relevant topics for further research. The first topic would be to include rider heterogeneity in the modelling. Here it will be a barrier that bike flow data is necessary to correct for exposure. These flow data will be difficult to collect together with socio-demographic information and indicators of risky cyclists. Therefore it necessitates a combined effort of modelling and data collection advances to gain knowledge about heterogeneity in the bike flows. However, given heterogeneous flow data, the Palm approach would allow for the inclusion of additional dimensions into the analysis of factors leading to higher bicycle crash risk. Other factors that more easily could be included in future studies would be information on bicycle infrastructure. In the current data, these were not available, but it should be possible to include them in future work, which would allow for an investigation of interaction effects between infrastructure and weather.

CRediT authorship contribution statement

Marcus Skyum Myhrmann: Conceptualization, Data management, Formal analysis, Visualization, Writing – original draft, Writing – review & editing. **Stefan Eriksen Mabit:** Conceptualization, Formal analysis, Writing – review & editing.

Declaration of competing interest

The authors declare that they have no known competing financial interests or personal relationships that could have appeared to influence the work reported in this paper.

Data availability

The authors do not have permission to share data.

Acknowledgements

We thank Marco Dozza, Greg Fountas and Carlos Azevedo for valuable feedback on an earlier version of the paper. We are also grateful to three anonymous reviewers for their useful comments that helped us improve the paper.

References

Abdel-Aty, M., Ekram, A.A., Huang, H., Choi, K., 2011. A study on crashes related to visibility obstruction due to fog and smoke. Accid. Anal. Prev. 43 (5), 1730–1737. http://dx.doi.org/10.1016/j.aap.2011.04.003.

Aldred, R., Goodman, A., Gulliver, J., Woodcock, J., 2018. Cycling injury risk in London: A case-control study exploring the impact of cycle volumes, motor vehicle volumes, and road characteristics including speed limits. Accid. Anal. Prev. 117, 75–84. http://dx.doi.org/10.1016/J.AAP.2018.03.003.

Andrey, J., Yagar, S., 1993. A temporal analysis of rain-related crash risk. Accid. Anal. Prev. 25 (4), 465–472. http://dx.doi.org/10.1016/0001-4575(93)90076-9.

Asgarzadeh, M., Fischer, D., Verma, S.K., Courtney, T.K., Christiani, D.C., 2018. The impact of weather, road surface, time-of-day, and light conditions on severity of bicycle-motor vehicle crash injuries. Am. J. Ind. Med. 61 (7), 556–565. http://dx.doi.org/10.1002/AJIM.22849.

Bishop, C.M., 1994. Mixture Density Networks. Technical Report, Aston University, URL: http://www.ncrg.aston.ac.uk/.

Clopper, C.J., Pearson, E.S., 1934. The use of confidence or fiducial limits illustrated in the case of the binomial. Biometrika 26 (4), 404–413. http://dx.doi.org/10.1093/biomet/26.4.404.

Danmarks Statistik, 2021. Injured in road traffic accidents reported by casualty wards by reporter, accident situation, means of transport, sex, age and casualty (classified by diagnosis) - StatBank Denmark - data and statistics. URL: https://statbank.dk/statbank5a/SelectVarVal/Define.asp?MainTable=MOERKE1&PLanguage=1&PXSId=0&wsid=cftree.

DMI, 2021. Danish meteorological institute - open data - DMI open data - confluence. URL: https://confluence.govcloud.dk/display/FDAPI/Danish+Meteorological+Institute+-+Open+Data.

Dozza, M., 2017. Crash risk: How cycling flow can help explain crash data. Accid. Anal. Prev. 105, 21–29. http://dx.doi.org/10.1016/J.AAP.2016.04.033.

Elvik, R., 2009. The non-linearity of risk and the promotion of environmentally sustainable transport. Accid. Anal. Prev. 41 (4), 849–855. http://dx.doi.org/10.1016/J.AAP.2009.04.009.

Elvik, R., Bjørnskau, T., 2017. Safety-in-numbers: A systematic review and meta-analysis of evidence. Saf. Sci. 92, 274–282. http://dx.doi.org/10.1016/J.SSCI.2015.07.017.

Gustafsson, L., Archer, J., 2013. A naturalistic study of commuter cyclists in the greater stockholm area. Accid. Anal. Prev. 58, 286–298. http://dx.doi.org/10.1016/j.aap.2012.06.004.

Heaton, K., 2009. Sleep and motor vehicle crash risk. J. Emerg. Nurs. 35 (4), 363–365. http://dx.doi.org/10.1016/j.jen.2009.02.012.

Hochreiter, S., Schmidhuber, J., 1997. Long short-term memory. Neural Comput. 9 (8), 1735–1780. http://dx.doi.org/10.1162/neco.1997.9.8.1735.

Horton, D., 2016. Fear of cycling. In: Cycling and Society. Routledge, pp. 149–168. http://dx.doi.org/10.4324/9781315575735-13.

Infrastructures, M.d.D.d.e.d., 2015. Declaration on Cycling as a climate friendly Transport Mode Preamble. Technical Report, URL: www.gouvernement.lu.

Janstrup, K.H., Kaplan, S., Hels, T., Lauritsen, J., Prato, C.G., 2016. Understanding traffic crash under-reporting: Linking police and medical records to individual and crash characteristics. Traffic Inj. Prev. 17 (6), 580–584. http://dx.doi.org/10.1080/15389588.2015.1128533.

Kim, J.-K., Kim, S., Ulfarsson, G.F., Porrello, L.A., 2007. Bicyclist injury severities in bicycle–motor vehicle accidents. Accid. Anal. Prev. 39 (2), 238–251. http://dx.doi.org/10.1016/J.AAP.2006.07.002.

Lord, D., Mannering, F., 2010. The statistical analysis of crash-frequency data: A review and assessment of methodological alternatives. Transp. Res. A 44 (5), 291–305. http://dx.doi.org/10.1016/J.TRA.2010.02.001.

Malin, F., Norros, I., Innamaa, S., 2017. Accident risk of road and weather conditions on different road types. In: Road Safety & Simulation International Conference 2017, Vol. 122. Elsevier, pp. 181–188. http://dx.doi.org/10.1016/j.aap.2018.10.014.

Malyshkina, N.V., Mannering, F.L., Tarko, A.P., 2009. Markov switching negative binomial models: An application to vehicle accident frequencies. Accid. Anal. Prev. 41 (2), 217–226. http://dx.doi.org/10.1016/j.aap.2008.11.001.

Mannering, F., Bhat, C., 2014. Analytic methods in accident research: Methodological frontier and future directions. Anal. Methods Accid. Res. 1, 1–22. http://dx.doi.org/10.1016/j.amar.2013.09.001.

Mannering, F., Bhat, C.R., Shankar, V., Abdel-Aty, M., 2020. Big data, traditional data and the tradeoffs between prediction and causality in highway-safety analysis. Anal. Methods Accid. Res. 25, 100113. http://dx.doi.org/10.1016/J.AMAR.2020.100113.

Miranda-Moreno, L.F., Strauss, J., Morency, P., 2011. Disaggregate exposure measures and injury frequency models of cyclist safety at signalized intersections. Transp. Res. Rec. 2236 (1), 74–82. http://dx.doi.org/10.3141/2236-09.

Møller, M., Janstrup, K.H., Pilegaard, N., 2021. Improving knowledge of cyclist crashes based on hospital data including crash descriptions from open text fields. J. Saf. Res. 76, 36–43. http://dx.doi.org/10.1016/j.jsr.2020.11.004.

Mueller, N., Rojas-Rueda, D., Cole-Hunter, T., de Nazelle, A., Dons, E., Gerike, R., Götschi, T., Int Panis, L., Kahlmeier, S., Nieuwenhuijsen, M., 2015. Health impact assessment of active transportation: A systematic review. Prev. Med. 76, 103–114. http://dx.doi.org/10.1016/J.YPMED.2015.04.010.

Myhrmann, M.S., Janstrup, K.H., Møller, M., Mabit, S.E., 2021. Factors influencing the injury severity of single-bicycle crashes. Accid. Anal. Prev. 149, 105875. http://dx.doi.org/10.1016/j.aap.2020.105875.

Myhrmann, M.S., Mabit, S.E., 2023. Estimating city-wide hourly bicycle flow using a hybrid LSTM MDN. Transportation Research Part A 176, 103783. http://dx.doi.org/10.1016/j.tra.2023.103783.

Næss, I., Galteland, P., Skaga, N.O., Eken, T., Helseth, E., Ramm-Pettersen, J., 2020. The number of patients hospitalized with bicycle injuries is increasing - a cry for better road safety. Accid. Anal. Prev. 148, 105836. http://dx.doi.org/10.1016/j.aap.2020.105836.

Norros, I., Kuusela, P., Innamaa, S., Pilli-Sihvola, E., Rajamäki, R., 2016. The palm distribution of traffic conditions and its application to accident risk assessment. Anal. Methods Accid. Res. 12 (March), 48–65. http://dx.doi.org/10.1016/j.amar.2016.10.002.

Pack, A.I., Pack, A.M., Rodgman, E., Cucchiara, A., Dinges, D.F., Schwab, C.W., 1995. Characteristics of crashes attributed to the driver having fallen asleep. Accid. Anal. Prev. 27 (6), 769–775. http://dx.doi.org/10.1016/0001-4575(95)00034-8.

Paulsen, M., Nagel, K., 2019. Large-scale assignment of congested bicycle traffic using speed heterogeneous agents. In: Procedia Computer Science, Vol. 151. Elsevier B.V., pp. 820–825. http://dx.doi.org/10.1016/j.procs.2019.04.112.

Prato, C.G., Rasmussen, T.K., Nielsen, O.A., Watling, D.P., 2013. A disaggregate pseudo-dynamic assignment for the activity-based model of the Greater Copenhagen Area. In: WCTR 2013: 13th World Conference on Transportation Research, Rio de Janeiro, Brazil, 15-18 July 2013.

Roos, J., Lindqvist, S., 2020. Identifiering av områden med förhöjd olycksrisk för cyklister baserad på cykelhjälmsdata. In: Technical Report. Malmö University, URL: http://muep.mau.se/handle/2043/32083.

von Stülpnagel, R., Petinaud, C., Liß ner, S., 2022. Crash risk and subjective risk perception during urban cycling: Accounting for cycling volume. Accid. Anal. Prev. 164, 106470. http://dx.doi.org/10.1016/J.AAP.2021.106470.

TomTom International BV, 2021. Copenhagen traffic report | TomTom traffic index. URL: https://www.tomtom.com/en_gb/traffic-index/copenhagen-traffic/.

Transport for London, 2014. Attitudes Towards Cycling Annual Report 2014 TfL. Technical Report, Transport for London, pp. 1–198, URL: https://tfl.gov.uk/cdn/static/cms/documents/attitudes-to-cycling-2014-report.pdf.

Useche, S.A., Montoro, L., Alonso, F., Oviedo-Trespalacios, O., 2018a. Infrastructural and human factors affecting safety outcomes of cyclists. Sustainability 10 (2), 86–95. http://dx.doi.org/10.3390/su10020299.

Useche, S.A., Montoro, L., Alonso, F., Tortosa, F.M., 2018b. Does gender really matter? A structural equation model to explain risky and positive cycling behaviors. Accid. Anal. Prev. 118, 86–95. http://dx.doi.org/10.1016/j.aap.2018.05.022.

Vandenbulcke, G., Thomas, I., Int Panis, L., 2014. Predicting cycling accident risk in Brussels: A spatial case–control approach. Accid. Anal. Prev. 62, 341–357. http://dx.doi.org/10.1016/J.AAP.2013.07.001.

Vanparijs, J., Int Panis, L., Meeusen, R., de Geus, B., 2015. Exposure measurement in bicycle safety analysis: A review of the literature. Accid. Anal. Prev. 84, 9–19. http://dx.doi.org/10.1016/j.aap.2015.08.007.

Vanparijs, J., Int Panis, L., Meeusen, R., de Geus, B., 2016. Characteristics of bicycle crashes in an adolescent population in Flanders (Belgium). Accid. Anal. Prev. 97, 103–110. http://dx.doi.org/10.1016/j.aap.2016.08.018.

Vejdirektoratet, 2018. Hvorfor Stiller Vi Cyklen? Technical Report, Vejdirektoratet, Copenhagen, p. 16.

Williams, T., 2015. Investigating Characteristics in a Spatial Context That Contribute to Where Bicycle Accidents Occur (Ph.D. thesis). Lincoln University, p. 115, URL: https://researcharchive.lincoln.ac.nz/bitstream/handle/10182/6847/Williams_MApplSc.pdf?isAllowed=y&sequence=6.

Yu, R., Abdel-Aty, M., Ahmed, M., 2013. Bayesian random effect models incorporating real-time weather and traffic data to investigate mountainous freeway hazardous factors. Accid. Anal. Prev. 50, 371–376. http://dx.doi.org/10.1016/j.aap.2012.05.011.